IOP Conference Series: Earth and Environmental Science

PAPER • **OPEN ACCESS**

Predicting the shear modulus and damping ratio of soils using machine learning models

To cite this article: M Bayat *et al* 2024 *IOP Conf. Ser.: Earth Environ. Sci.* **1334** 012040

Predicting the shear modulus and damping ratio of soils using machine learning models

M Bayat [1,2*], Z Mousavi [2] and W W Feng[2,3]

[1]Department of Civil Engineering, Najafabad Branch, Islamic Azad University, Najafabad, Iran
[2]Department of Ocean Science and Engineering, Southern University of Science and Technology, Shenzhen, China
[3]Southern Marine Science and Engineering Guangdong Laboratory (Guangzhou), Guangzhou, China

*Corresponding author: bayat.m@pci.iaun.ac.ir

Abstract. In geotechnical engineering, the accurate estimation of fundamental soil properties, such as the shear modulus ratio ($G/G_{\max}$) and damping ratio (D), is crucial to design and analyze various structures subjected to dynamic loads. This study presents a comprehensive investigation on harnessing the power of machine learning techniques to precisely predict $G/G_{\max}$ and D of granular soils. Using an extensive dataset gathered from cyclic triaxial and resonant column tests on diverse mixtures of sand and gravel, combined with previous research findings, a series of advanced machine learning algorithms including shallow neural networks, support vector regression, gradient boosting regression, and deep feed forward neural network (DFFNN) were developed. The proposed models elucidate various influential parameters, including the grading characteristics, void ratio, confining pressure, consolidation stress ratio, and specimen preparation techniques. The superiority of the DFFNN model in terms of accuracy and predictive performance was demonstrated through rigorous evaluation and comparison. This study contributes to a better understanding of soil behavior under dynamic conditions. It also provides a robust framework to employ machine learning in predicting $G/G_{\max}$ and D of granular soils, thereby enhancing the efficiency and reliability of geotechnical designs and construction practices.

1. Introduction

This section emphasizes the importance of understanding the dynamic behavior of geomaterials, particularly granular soils, in designing safe structures. Two key parameters, the shear modulus ratio ($G/G_{\max}$) and damping ratio (D), are considered crucial for characterizing the dynamic response of these soils [1–4]. Complex testing methods are used to determine the dynamic soil properties. Integrating artificial intelligence (AI) and machine learning (ML), particularly deep learning (DL), into geotechnical engineering has been introduced as a transformative development.

ML, a subfield of AI, is described as a field that enables machines to learn from data and make predictions, thereby revolutionizing various engineering disciplines. Different ML methods, such as supervised, unsupervised, semi-supervised, and reinforcement learning methods, are briefly explained in references [5–7].

DL, a subset of ML, has been highlighted for its ability to process large datasets with high-dimensional features and the potential of artificial neural networks (ANNs) for modeling data is discussed. The application of ML in geotechnical engineering is considered innovative because it enables accurate analysis and prediction of soil behavior, foundation performance, and slope stability [8–10].

Previous studies focused on classifying soils, estimating the dynamic properties of soils, and predicting the shear strength. This study discusses the use of various ML methods, including ANNs, support vector regression (SVR), and gradient boosting regression (GBR), for different geotechnical applications and demonstrates their effectiveness in producing accurate predictions.

This study investigates the influence of several factors on the dynamic properties of sand-gravel mixtures and compares the prediction performance of the deep feed forward neural network (DFFNN) model with that of other ML models. A dataset of 118 curves was used for training and testing, and sensitivity analysis was performed to evaluate the importance of the input parameters.

2. Machine learning models

This section provides an overview of the machine-learning models, including ANN, SVR, and GBR.

2.1. ANNs and deep feed forward neural networks

ANNs have been applied in geotechnical engineering to classify soils, predict slope stability, and assess risks. They consist of interconnected layers of neurons, including the input, output, and hidden layers. DFFNNs were introduced as variants of ANNs that are designed to address the limitations of slow convergence rates and overfitting [11–13]. DFFNNs can effectively learn and represent complex data patterns and relationships. They comprise feed-forward and backpropagation stages, and often include dropout and batch normalization (BN) layers to prevent overfitting and expedite training, respectively. Activation and loss functions having various available options are used in DFFNNs. DFFNNs aim to convert input data into desired outputs by accommodating both linear and nonlinear relationships.

2.2. SVR

SVR is a technique derived from a support vector machine (SVM) that was initially designed for classification but has found applications in regression tasks. SVR employs a mapping function to transform input variables into a higher-dimensional feature space, where linear regression is performed. The goal of SVR is to determine a function that approximates the output values with a satisfactory level of precision. The SVR model is based on weight vectors, bias, and independent observations [14–16].

2.3. GBR

GBR, which is an ensemble ML technique, addresses regression challenges. It utilizes multiple decision trees in its framework and progressively reduces the residuals in each ensemble tree, thereby iteratively enhancing the model [17,18]. GBR operates on a boosting methodology using a collection of high-bias and low-variance models to simultaneously reduce bias and maintain low variance [19,20]. Each decision tree partitions the input space into separate regions and assigns constant values to each region. The model aims to minimize the loss function using various available options, such as the Huber loss function, absolute error, squared error, and mean squared error (MSE). In this study, MSE was chosen as the loss function.

2.4. Developed DFFNN model

A DFFNN model was designed in this study using the Keras library in Python to extract desired features and predict $G/G_{\max}$ and D values of granular soils based on their physical and geotechnical properties. The architecture of the DFFNN model comprises six fully connected (FC) layer blocks, the design of which is detailed in table 1.

Table 1. Details of the proposed architecture model.

Type of layer	Activation function	Number of neurons	Outputs
FC	Relu	30	(None, 30)
FC	Relu	20	(None, 20)
FC	Relu	15	(None, 15)
FC	Relu	10	(None, 10)
FC	Relu	5	(None, 5)
FC	Linear	2	(None, 2)

The DFFNN model architecture is as follows:

1. A dropout layer,
2. An FC layer with a rectified linear unit (Relu) activation function and batch normalization (BN) layer,
3. The architecture of the previous stage was repeated four more times and,
4. The output of the previous architecture was connected to the FC layer to calculate the outputs.

The hyperparameters of the DFFNN model were adjusted to improve the optimal convergence rate. The training procedure was completed with a batch size of 100 and learning rate of 0.001. A Nadam optimizer was employed in the DFFNN model to iteratively adjust the network parameters and minimize the loss function.

The loss function used in the model comprised the sum of the MSE term and a regularization term, which was defined as the L1- and L2-norms of the network weights, denoted as λ_1 and λ_2, respectively. These hyperparameters were used to control the complexity of the model. Table 2 lists the ideal hyperparameters for the proposed DFFNN model.

This model was developed to accurately predict the $G/G_{\max}$ and D values of granular soils based on the input data, and hyperparameter tuning was aimed at optimizing the performance and convergence of the model.

In this study, 2,844 samples were analyzed. To train and evaluate the proposed model, the dataset was divided as follows:

1. 70% (1,991 samples) were allocated for training.
2. 10% (284 samples) were used for validation.
3. 20% (569 samples) were used for testing.

The input parameters were normalized to ensure that the data had consistent scales, which is a critical step in modeling, particularly when the inputs have varying scales. Z-score normalization was chosen for stability, even in the presence of outliers. This technique involves dividing the value by standard deviation (σ) after subtracting the mean (μ). The scaled value (Z) was related to the original value (X) through the following equation:

$$Z = (X - \mu)/\sigma \tag{1}$$

This normalization process was applied to the training dataset and the same scale (μ and σ) was used to normalize the testing dataset. This approach facilitates model generalization and domain adaptation.

Domain adaptation is a challenging problem, particularly when predicting samples from a different working environment (target domain) using a model trained on samples from another environment (source domain). This is commonly referred to as a domain-adaptation problem. Normalizing the

datasets ensures that the model can adapt to different domains and make accurate predictions even when the source and target domains differ.

Table 2. Optimal hyperparameters employed for the developed DFFNN model.

Hyper-Parameters	Search space	Optimal value
Optimizer	RMSProp, Adam, SGD, Nadam	Nadam
Learning Rate	0.01,0.001,0.0001	0.001
The number of FC layers	2,6,8,10	6
Activation function in the hidden FC layers	Relu, Leaky-Relu, Logsig, Tansig	Relu
No. neurons in the first FC layer	30,20,15,10,5	30
No. neurons in the second FC layer	30,20,15,10,5	20
No. neurons in the third FC layer	30,20,15,10,5	15
No. neurons in the fourth FC layer	30,20,15,10,5	10
No. neurons in the fifth FC layer	30,20,15,10,5	5
Batch Size	4,8,10,16,32,64,100	100
Dropout Ratio	0,0.2,0.3,0.4,0.5	0.2
λ_1 and λ_2	0.1,0.01,0.001	0.01

2.5. Performance evaluation

The performance of the models was evaluated to assess their predictive accuracy. Two key statistical metrics were used, namely R^2 and MAE. The R^2 indicates the relationship between the observed and predicted values and MAE quantifies the average absolute difference between the observed and predicted values. A model with R^2 and MAE values of 1 and 0, respectively, is considered to be ideal. These metrics were used to gauge the proficiency and accuracy of the constructed models.

3. Dataset collection

A comprehensive series of resonant column (RC) and cyclic triaxial (CT) tests were performed in this study to investigate the dynamic properties of soils. These tests aimed to provide a detailed understanding of the behavior of soil specimens under varying conditions and shear strain amplitudes. The specific details of these tests and materials are as follows.

To investigate the impact of various factors on the dynamic properties of soils, a set of RC and CT tests was conducted on reconstituted specimens of sand-gravel mixtures. The parameters considered included gravel content, relative density, mean confining pressure, consolidation stress ratio, and the method used to prepare the specimens. The sand used in this study was clean, finely graded had minimal silt content, and classified as poorly graded sand (SP) according to the unified soil classification system (USCS). In contrast, the gravel material was uniformly graded with particle sizes ranging from 15 mm to 4.75 mm. Five groups of granular soil with different gravel contents were used. Figure 1 shows the grain size distribution curves.

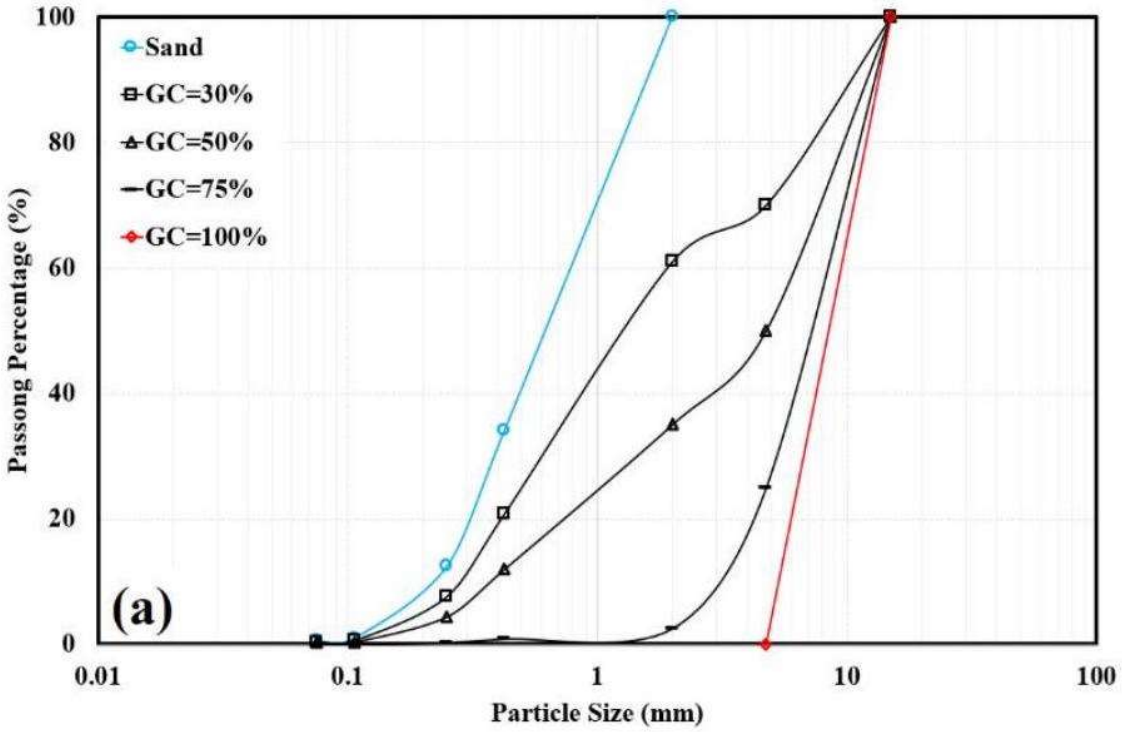

Figure 1. Grain size distribution curves.

To prepare the soil specimens for the RC and CT tests, cylindrical specimens measuring 10 cm and 20 cm in diameter and height, respectively, were carefully created using wet tamping, air pluviation, and water sedimentation techniques. The experimental procedures and methodologies for specimen preparation are described in detail by Bayat and Ghalandarzadeh [4].

RC and CT testing apparatuses were used to assess the dynamic characteristics over a range of shear-strain amplitudes. These devices allow the application of consolidation stress during the consolidation phase, accommodating both isotropic and anisotropic stress conditions. Anisotropic stress was applied using the consolidation stress ratio (ratio of lateral to axial effective consolidation stress). CT tests focused on dynamic properties within moderate to substantial shear strain amplitudes, typically ranging from $10^{\wedge-4}$ to $10^{\wedge-2}$. RC tests, on the other hand, characterize the dynamic properties within the lower to intermediate shear-strain amplitude range, spanning approximately $10^{\wedge-6}$ to $10^{\wedge-4}$.

The CT experiments followed the ASTM D-3999 guidelines. In this study, linear variable differential transducers (LVDTs) were attached to opposing sides of the triaxial specimens to monitor the average local axial strain. The loading phase included consistent cyclic shear-stress amplitudes that progressively increased. Each loading stage consisted of 40 loading cycles with uniform sinusoidal waveforms at a constant frequency of 1 Hz for the cyclic axial loading. The tests were performed under undrained conditions, with the excess pore water pressure dissipated before each loading phase. A detailed analysis of the hysteresis loop was performed at the tenth cycle within each stage to determine the values of G and D. G was calculated as the slope of the secant line connecting the hysteresis loop extremities, whereas D was computed based on the ratio of the energy dissipated during the loading cycle to the maximum strain energy stored throughout the cycle.

A free-free RC apparatus was used to assess small shear-strains in the range of $10^{\wedge-6}$ to $10^{\wedge-4}$. This apparatus induces torsional excitation to initiate the vibration of a cylindrical specimen, and enables rotational resonant frequency determination. The precision of the RC apparatus was established through a calibration process using aluminum calibration bars. The free-free resonant frequency method, known for its simplicity and utility among researchers, was adopted to measure the small-strain dynamic properties.

In the current study, a series of RC and CT tests was done to study the effects of gravel content (GC), mean effective confining pressure (σ'_m), void ratio (e), anisotropic consolidation ratio (K_c), and Specimens' Preparation (S-P) technique on the $G/G_{\max} - \gamma$ and $D - \gamma$ curves of sand-gravel mixtures. These parameters have important effects on the dynamic properties of granular materials.

4. Results and discussion

4.1. Performance of the proposed method in predicting G/G_{max} and D

The performance of the developed DFFNN model in predicting the combined outputs ($G/G_{\max}$ or D) was assessed by monitoring the variation in accuracy R^2 and MSE with respect to the number of training iterations on both the training and validation datasets, as shown in figure 2.

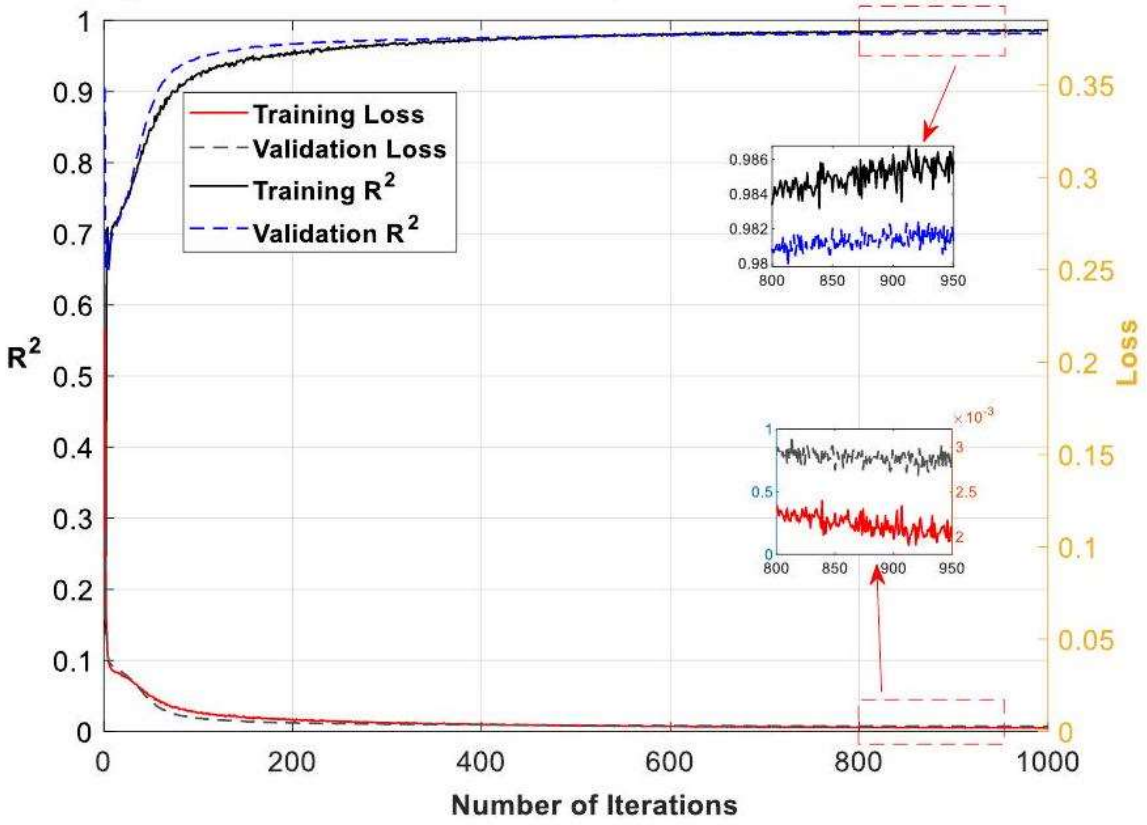

Figure. 2. Variation of R^2 and loss of the developed DFFNN model with respect to the number of iterations on training and validation datasets.

By the 600^{th} iteration, the accuracy of the developed DFFNN model reached a steady state with an impressive value of approximately 98%. Simultaneously, the loss of the model decreased significantly from 0.21 to 0.0025, indicating improved performance of the model.

A comparison of the R^2 and MAE of both the output parameters ($G/G_{\max}$ and D), for the predictions of the developed DFFNN model across the training, validation, and testing datasets is presented in table 3.

For the testing data, the DFFNN model achieved values of 0.9830 and 0.9396 for $G/G_{\max}$ and D, respectively, and MAE values of 0.0164 and 0.0069 for $G/G_{\max}$ and D, respectively. These results demonstrate that the model can effectively predict both the output parameters simultaneously with a relatively high level of accuracy, making it a valuable tool for geotechnical engineering applications.

Table 3. Comparison of R^2 and MAE of the developed DFFNN model for predicting both the output parameters based on training, validation, and testing datasets.

Output	Dataset	Mean Absolute Error (MAE)	Correlation Coefficient ($\mathbf{R^2}$)
D	Training	0.0063	0.9716
	Validation	0.0075	0.9618
	Testing	0.0069	0.9396
$G/G_{\max}$	Training	0.0131	0.9852
	Validation	0.0165	0.9816
	Testing	0.0164	0.9830
Combined outputs	Training	0.0099	0.9868
	Validation	0.0120	0.9818
	Testing	0.0114	0.9820

Figure 3 shows the predicted values of $G/G_{\max}$ and D from the DFFNN model plotted against the measured values for these parameters based on training, validation, and testing datasets. The results demonstrate the accuracy of the model in predicting geotechnical properties.

Figure 3(a) shows that the DFFNN model can accurately predict $G/G_{\max}$ and D for granular soils using the training dataset and achieve high determination correlation coefficient R^2 of 0.9852 for $G/G_{\max}$ and 0.9716 for D. The MAE values were 0.0131 for $G/G_{\max}$ and 0.0063 for D, which indicates excellent predictive performance for this dataset that contains 1,991 data points.

When the trained DFFNN model was applied to predict $G/G_{\max}$ and D in the validation (284 data points) and testing datasets (569 data points), it continued to exhibit high accuracy for $G/G_{\max}$ prediction, as reflected in the correlation coefficients ($R^2 = 0.9816$ for the validation dataset and $= 0.9830$ for the testing dataset) and the corresponding MAE values (0.0165 for the validation dataset and 0.0164 for the testing dataset). The model showed moderate accuracy in predicting D, with correlation coefficients R^2 of 0.9618 for the validation dataset and 0.9396 for the testing dataset, along with corresponding MAE values of 0.0075 and 0.0069, respectively.

The developed DFFNN model demonstrated consistent and accurate performance in predicting $G/G_{\max}$ across different datasets and the predicted data closely aligned with the line of equity (1:1 line). The majority of data points were within the 20% error range.

Figure 4 illustrates the residual errors of the DFFNN model between the measured and predicted values of $G/G_{\max}$ and D for the training, validation, and testing datasets. Residual errors represent the differences between the measured and predicted values. It is evident that the frequency of the residual errors near zero is high, indicating that the model makes accurate predictions.

The mean values (μ) and standard deviations (σ) of $G/G_{\max}$ and D for the testing dataset are also depicted in figure 4. For $G/G_{\max}$, the mean value and standard deviation is -0.0016 and 0.0348, respectively. For D, the mean value and standard deviation is -0.0003 and0.0127, respectively. These low standard deviations demonstrate the ability of the model to predict $G/G_{\max}$ and D of granular soils with precision and reliability.

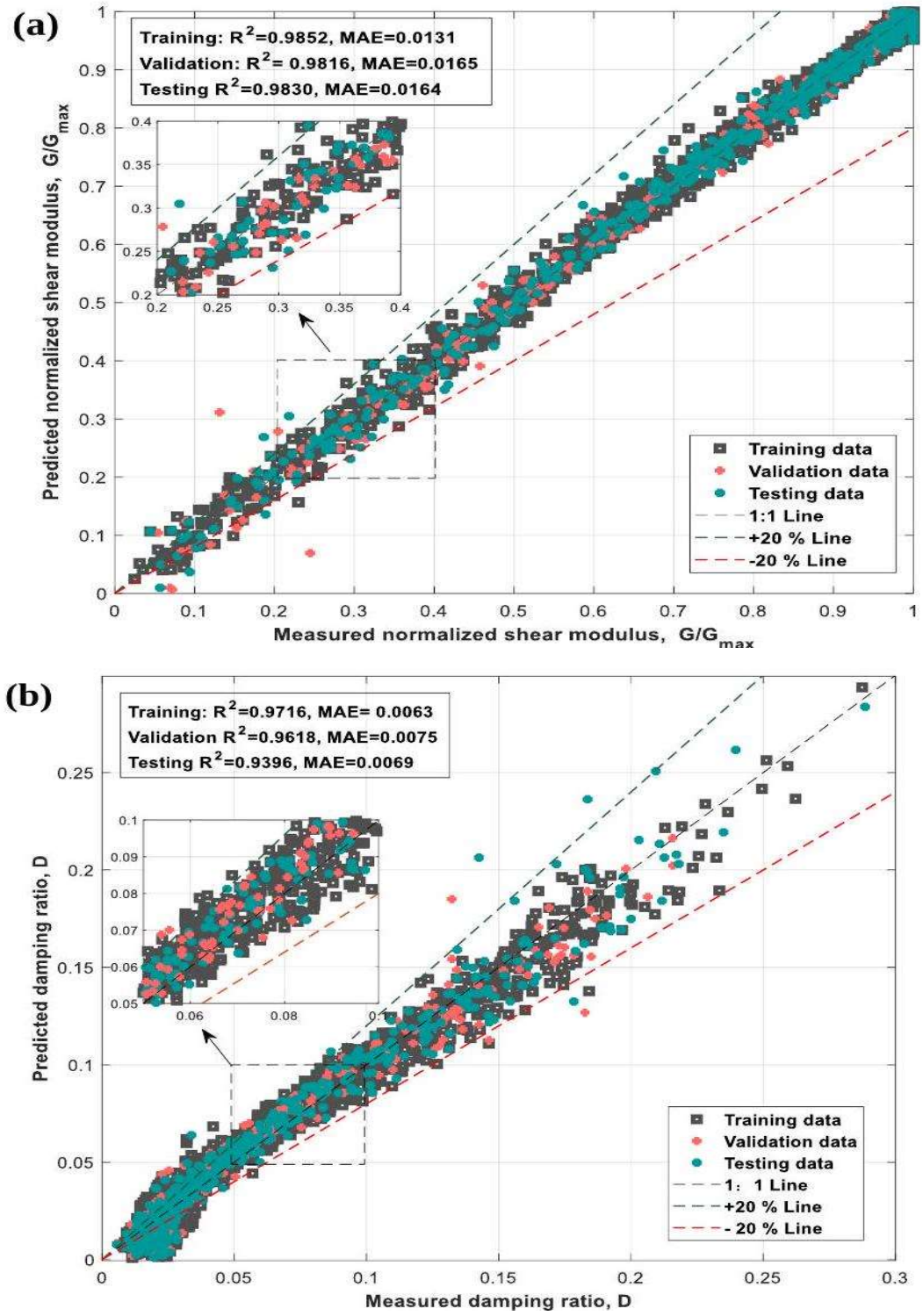

Figure 3. Measured and predicted results of the training, validation and testing datasets for performance evaluation of the developed DFFNN model in predicting (a) Normalized shear modulus (b) Damping ratio.

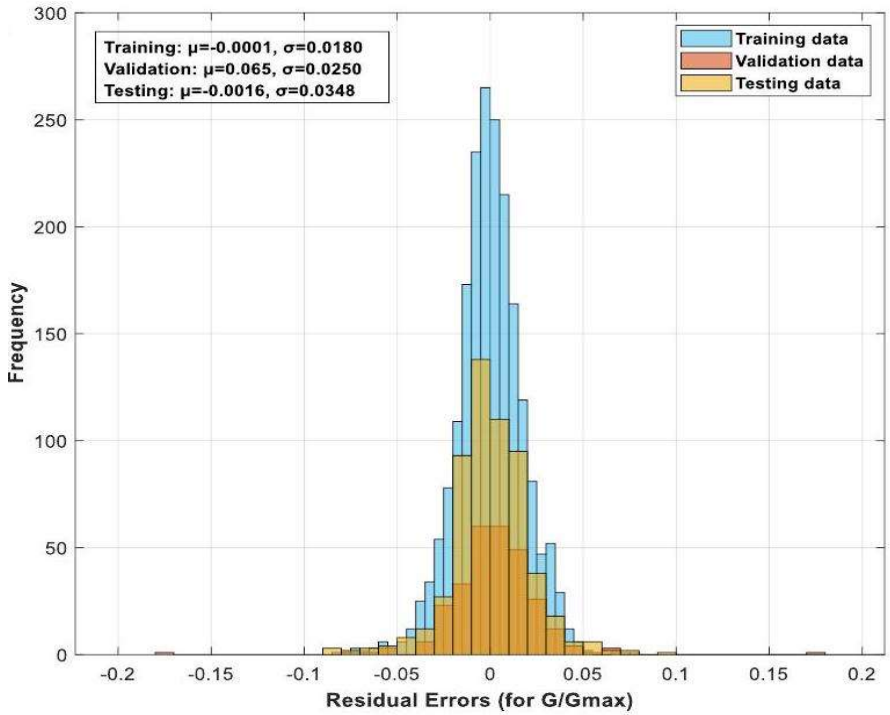

(a)

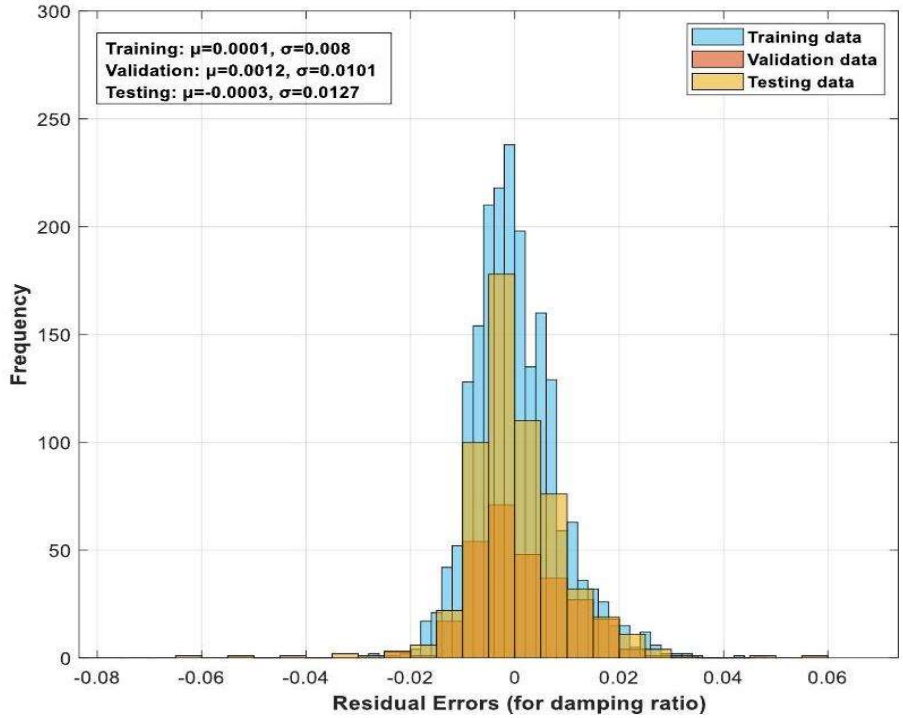

(b)

Figure 4. Distribution of the residual errors for the developed DFFNN model for (a) Normalized shear modulus (b) Damping ratio.

Figure 5 depicts a comparative analysis of the measured and predicted values of $G/G_{\max}$ and D using the developed DFFNN model across the training, validation, and testing datasets. This comparison helps assess the performance of the model across different datasets, and it is clear from the figure that the DFFNN model consistently provides accurate predictions and the predicted values closely match the measured values.

Figure 6 illustrates the measured and predicted $G/G_{\max} - \gamma$ and $D - \gamma$ curves for specific soil specimens under different conditions. Figure 6(a) displays the measured and predicted $G/G_{\max} - \gamma$ and $D - \gamma$ curves for pure sand specimens with $D_r = 10\%$ under mean confining pressure levels of 100,300 kPa and 600 kPa. These curves serve as an example of the overall results and show how the measured and predicted values of $G/G_{\max} - \gamma$ and $D - \gamma$ vary with shear-strain levels. The results indicate that the predicted values for both parameters at shear-strain levels greater than $10^{\wedge -2}$ are more accurate than those at smaller strain levels. This can be attributed to errors in measuring the dynamic parameters at small strain levels, which are inherent to measurement devices operating within this range. Understanding the soil behavior at small strain levels is essential for the foundation design and construction methods and for predicting the settlement and structural response to minor ground vibrations. At medium strain levels, dynamic parameters are crucial for assessing the soil liquefaction potential during moderate seismic events. These parameters are also indispensable for predicting soil failure and deformation during major seismic events at large strain levels.

However, it is important to note that measuring the soil dynamic parameters using tests such as RC and CT can introduce errors and uncertainties into the results. The magnitude of these errors depends on various factors, including the specific test method, equipment, soil conditions, and operator experience. However, tests conducted at smaller strain levels, particularly in the small-to-medium strain regime, tended to exhibit a higher degree of measurement error than tests at moderate-to-large strain levels. This suggests that obtaining precise measurements in the lower strain regime can be more challenging, potentially contributing to errors in predicting soil dynamic parameters at strain levels smaller than $10^{\wedge -2}$.

The results from the developed DFFNN model highlight its effectiveness in predicting soil dynamic parameters with high accuracy, particularly in granular soils and their behavior at different strain levels.

4.2. Shallow neural network (SNN) model

The SNN model was configured with 30-neurons in a hidden FC layer. The model parameters were systematically fine-tuned using an iterative trial-and-error approach to enhance convergence. Training used MSE as the cost function, which is a common choice in previous studies [78-80]. Network optimization was performed using the RMSProp optimizer with a learning rate of 0.001, batch size of 100, and maximum of 100 training epochs. The hidden FC layer featured a sigmoid activation function, whereas the last layer used a linear activation function.

4.3. SVR model

The SVR hyperparameters encompass parameters like the regularization parameter (C), error sensitivity parameter (ε), standard deviation (σ), and choice of kernel function. In this study, the gaussian radial basis function (RBF) was employed as the kernel function in SVR and they were fine-tuned using a grid search technique [21]. Initially, the hyperparameters C, ε, and σ were assigned a range of values as follows: C values of $0.1,1,10,100,1000$; ε values of $0.001,0.01,0.1$, 1; and σ values of $1,0.1,0.01,0.001,0.0001$. However, using the grid search technique, the optimal values for these hyperparameters were determined as 100 for $\mathrm{C}, 0.01$ for ε, and 1 for σ.

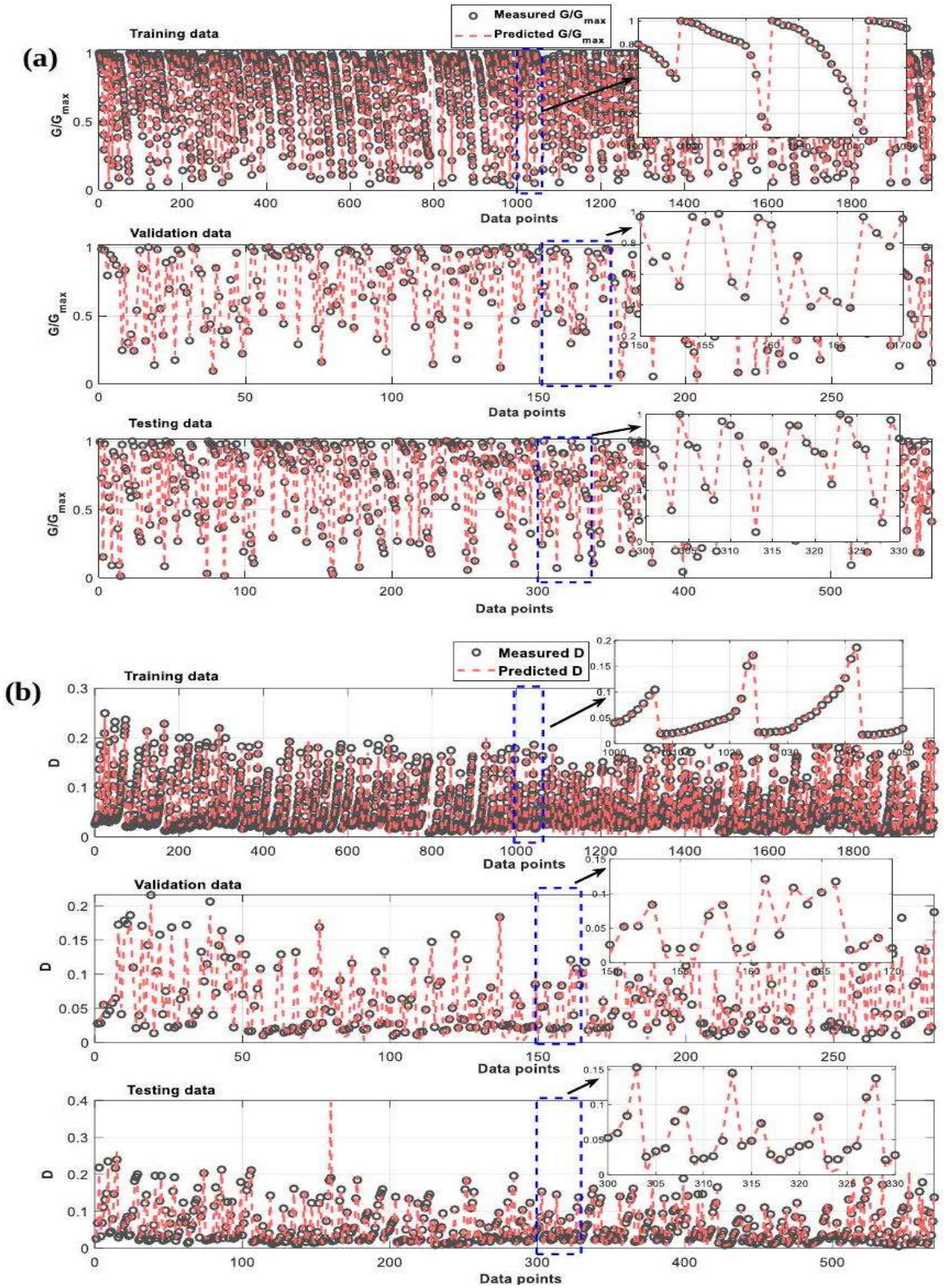

Figure 5. Measured values versus DFFNN predicted values for (a) Normalized shear modulus (b) Damping ratio.

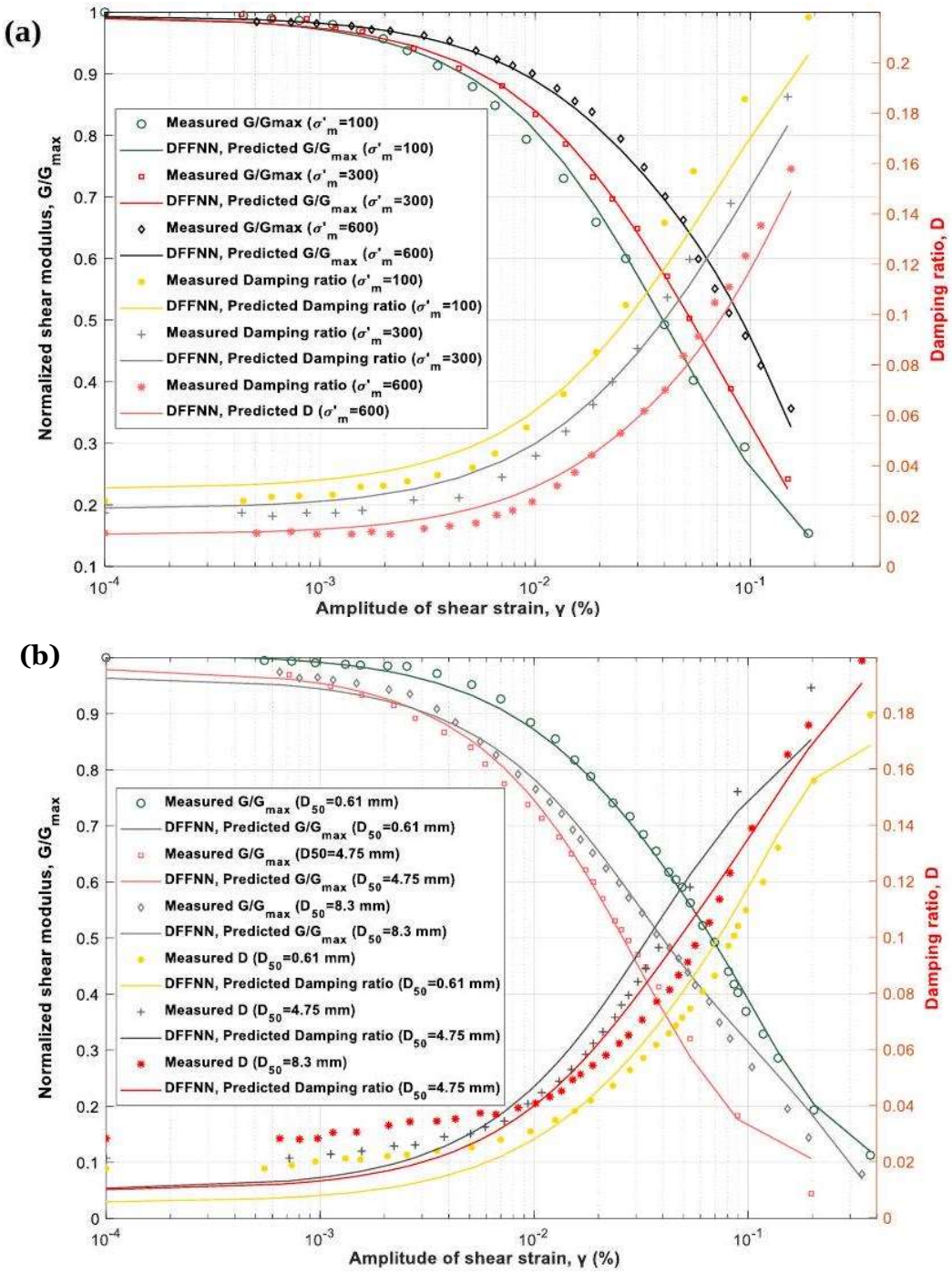

Figure 6. Measured values versus the predicted values of the normalized shear modulus and damping ratio (for testing dataset) by the DFFNN model, (a) GC = 0%, $D_r = 10\%$, (b) $\sigma'_m = 100$ kPa, $D_r = 60\%$.

4.4. GBR model

The hyperparameters of the GBR model were meticulously adjusted to optimize the convergence rate. The optimal settings for the GBR model, including the learning rate, number of trees, loss function, and maximum depth, were determined as 0.01,1300, MSE, and 21, respectively.

The Keras library in Python was used to implement the SNN, SVR, and GBR models. Their performances, evaluated on the testing dataset using all input parameters, are summarized in table 4 and

visually compared in figure 7. The results achieved by the proposed DFFNN model are highlighted in bold in table 4. According to the results, for predicting $G/G_{\max}$, the DFFNN attained a R^2 and MAE values of 0.9830 and 0.0164, respectively. In comparison, the respective R^2 and MAE values attained by GBR, SVR, and SNN are 0.9746 and 0.0761, 0.9162 and 0.0664, and 0.9173 and 0.0599, respectively. To predict D, the DFFNN delivered 0.9396 for R^2 and 0.0069 for MAE. In contrast, GBR yielded 0.9195 and 0.0083, SVR yielded 0.8568 and 0.0192, and SNN yielded 0.8416 and 0.0158, respectively.

These results highlight the superior prediction performance of the DFFNN, primarily because of its architectural capacity to automatically extract valuable features from input parameters. In addition, the GBR demonstrated strong performance, whereas the DFFNN and GBR excel in output prediction, SVR

SNN offers comparable performance. When comparing their accuracy in predicting $G/G_{\max}$ and D, it is evident that the $G/G_{\max}$ prediction is more precise, possibly because measuring the damping ratio in the laboratory is known to be more challenging and sensitive. Importantly, all the models achieved R^2 values above 0.90 and MAE below 0.07 for $G/G_{\max}$, while they attain R^2 above 0.80 and an MAE below 0.02 for D.

Table 4. Comparison of the R^2 and MAE of the different models using the testing dataset based on all input parameters.

Models	Output	All input parameters	
		MAE	$\overline{R^2}$
SNN	$G/G_{\max}$	0.0599	0.9173
	D	0.0158	0.8416
SVR	$G/G_{\max}$	0.0664	0.9162
	D	0.0192	0.8568
GBR	$G/G_{\max}$	0.0181	0.9746
	D	0.0083	0.9195
DFFNN	$G/G_{\max}$	0.0164	0.9830
	D	0.0069	0.9396

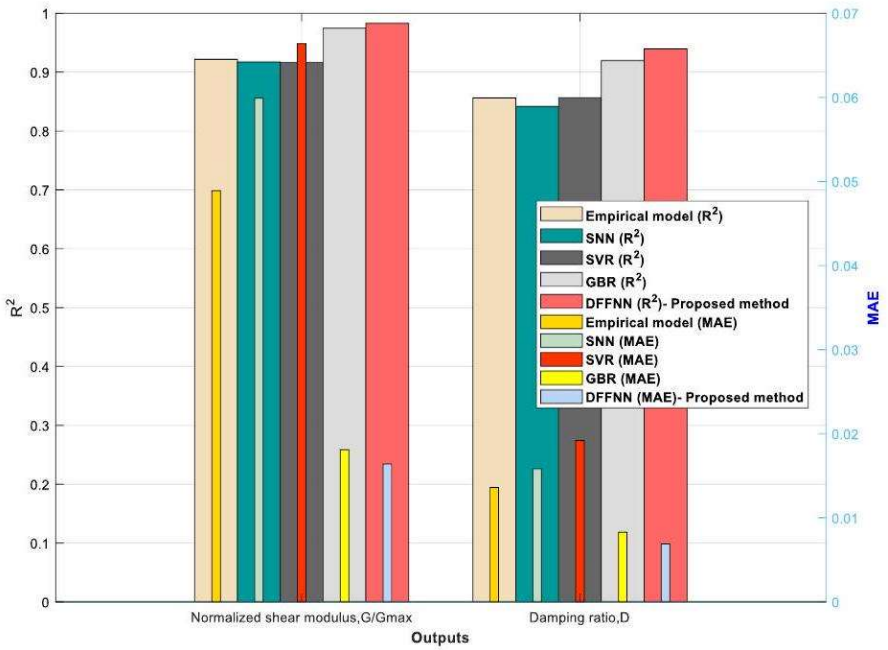

Figure 7. R^2 and MAE values of different models for predicting outputs using testing dataset.

5. Conclusion

An innovative approach was introduced for predicting the dynamic properties of geomaterials, specifically $G/G_{\max}$ and D. The proposed DFFNN model demonstrated a remarkable performance in predicting these parameters. By analyzing the accuracy and loss of the model during the training iterations, we observed that the DFFNN model achieved an impressive accuracy of approximately 98 % by the 600^{th} iteration. The loss of the model decreased significantly, highlighting its improved performance.

The assessment of the predictive capabilities of the model across different datasets, including training, validation, and testing, revealed a consistently high accuracy. For the testing data, the DFFNN model yielded correlation coefficients (R^2) of 0.9830 for $G/G_{\max}$ and 0.9396 for D, and low MAE values of 0.0164 for $G/G_{\max}$ and 0.0069 for D. These results demonstrate that the model can effectively predict both $G/G_{\max}$ and D with high accuracy, making it a valuable tool for geotechnical engineering applications. Comparative analyses of the measured and predicted values of $G/G_{\max}$ and D confirm the accuracy and consistency of the DFFNN model. It showed strong predictive performance for both parameters and remained accurate across different datasets, as is evident from the visual representations of the predicted values that closely aligned with the measured values.

In addition, the ability of the DFFNN model to accurately predict $G/G_{\max}$ and D across different shear-strain levels is noteworthy. It achieved high accuracy, particularly at shear-strain levels greater than $10^{\wedge-2}$, which is essential for understanding soil behavior in various geotechnical applications.

The performance of the DFFNN model was compared with that of other models, including SNN, SVR, and GBR. The DFFNN model outperformed these models primarily because of its architectural capacity to automatically extract valuable features from the input parameters. The GBR also showed strong performance in output prediction. While DFFNN and GBR excelled in output prediction, SVR and SNN provided comparable results. In summary, the remarkable accuracy and precision of the DFFNN model in predicting $G/G_{\max}$ and D makes it a valuable tool in geotechnical engineering. Its performance can aid in understanding soil behavior across different strain levels, which is essential for a wide range of geotechnical applications.

References

[1] Amir-Faryar B, Aggour M S and McCuen R H 2017 Universal model forms for predicting the shear modulus and material damping of soils *Geomech. Geoengin.* **12** 60–71
[2] Baghbani A, Choudhury T, Samui P and Costa S 2023 Prediction of secant shear modulus and damping ratio for an extremely dilative silica sand based on machine learning techniques. *Soil Dyn. Earthq. Eng.* **165** 107708
[3] Bayat M 2020 Universal model forms for predicting the dynamic properties of granular soils. *Acta Geodyn. Geomater.* 217–27
[4] Bayat M, Ghalandarzadeh A 2019 Influence of Depositional Method on Dynamic Properties of Granular Soil. *Int. J. Civ. Eng.* **17** 907–20
[5] Mousavi Z, Varahram S, Ettefagh M M and Sadeghi M H 2023 Dictionary learning-based damage detection under varying environmental conditions using only vibration responses of numerical model and real intact State: Verification on an experimental offshore jacket model. *MSSP* **182** 109567
[6] Mousavi Z, Ettefagh M M, Sadeghi M H and Razavi S N 2020 Developing deep neural network for damage detection of beam-like structures using dynamic response based on FE model and real healthy state. *Appl. Acoust.* **168** 107402
[7] Zhang W and Liu Z 2022 Editorial for machine learning in geotechnics. *Acta Geotech.* **17** 1017
[8] Choe D-E, Kim H-C and Kim M-H 2021 Sequence-based modeling of deep learning with LSTM and GRU networks for structural damage detection of floating offshore wind turbine blades. *Renew. Energy* **174** 218–35
[9] Das A, Chakrabortty P, Deb R and Banerjee S 2022 Prediction of large-strain cyclic behavior of clean sand using artificial neural network approach *Int. J. Adv. Eng. Sci. Appl. Math* **14** 60–79

[10] Zhang W, Li C, Peng G *et al.* 2018 A deep convolutional neural network with new training methods for bearing fault diagnosis under noisy environment and different working load *Mech. Syst. Signal Process* **100** 439–53
[11] Kardani N, Bardhan A, Gupta S *et al.* 2021 Predicting permeability of tight carbonates using a hybrid machine learning approach of modified equilibrium optimizer and extreme learning machine. *Acta Geotech.* 1–17
[12] Saadat M and Bayat M 2022 Prediction of the unconfined compressive strength of stabilised soil by Adaptive Neuro Fuzzy Inference System (ANFIS) and Non-Linear Regression (NLR). *Geomech. Geoengin.* **17**80–91
[13] Seventekidis P, Giagopoulos D, Arailopoulos A and Markogiannaki O 2020 Structural Health Monitoring using deep learning with optimal finite element model generated data. *Mech. Syst. Signal Process* **145** 106972
[14] HosseinAbadi HZ, Amirfattahi R, Nazari B, et al (2014) GUW-based structural damage detection using WPT statistical features and multiclass SVM. *Appl. Acoust.* **86** 59–70
[15] Santos P, Villa LF, Reñones A *et al.* 2015 An SVM-based solution for fault detection in wind turbines. *J. Sens.* **15** 5627–48
[16] Zhang X, Liang Y and Zhou J 2015 A novel bearing fault diagnosis model integrated permutation entropy, ensemble empirical mode decomposition and optimized SVM *Measurement* **69** 164179
[17] Bai X-D, Cheng W-C and Li G 2021 A comparative study of different machine learning algorithms in predicting EPB shield behaviour: a case study at the Xi'an metro, China *Acta Geotech*. **16** 4061–80
[18] Cheng W-C and Bai X-D EPB 2021 Shield behavior prediction using machine learning regression methods *The 2021 World Congress on Advances in Structural Engineering and Mechanics (ASEM21)* (GECE, Seoul, Korea)
[19] Ikeagwuani C C, Nwonu D C and Nweke C C 2022 Resilient modulus descriptive analysis and estimation for fine-grained soils using multivariate and machine learning methods *Int. J. Pavement Eng.* **23** 3409–24
[20] Kardani N, Aminpour M, Raja M N A *et al.* 2022 Prediction of the resilient modulus of compacted subgrade soils using ensemble machine learning methods *Transp. Geotech.* **36** 100827
[21] Syarif I, Prugel-Bennett A and Wills G 2016 SVM Parameter Optimization using Grid Search and Genetic Algorithm to Improve Classification Performance *TELKOMNIKA* **14** 1502